Deep-Sea Research, Vol. 29, No. 7A, pp. 869 to 882, 1982.
Printed in Great Britain.

0198–0149/82/070869–14 $03.00/0

Thermal changes in the western tropical Pacific in relation to the wind field

J. R. DONGUY*, C. HENIN*, A. MORLIERE* and J. P. REBERT*

(*Received* 5 *June* 1981; *in revised form* 2 *December* 1981; *accepted* 31 *January* 1982)

Abstract—Vertical displacement of the thermocline may be due either to a convergence or a divergence of Ekman transport in the surface layer. Data from ships of opportunity between New Caledonia and Japan are used to compute the wind stress curl, from 1973 to 1980, neglecting the zonal gradients. The pattern is compared to the changes of the 25°C isotherm depth between 5°N and 20°S from all data available between 160°E and 180°.

Alternate long periods of lifting and deepening of the thermocline appear in the western Pacific that may be roughly related to El Niño. Preceding El Niño the thermocline is deep in both the equatorial and the tropical western Pacific. The feature is due to the baroclinic response to the trade winds forcing on the equator associated with an Ekman convergence in the tropical zone. After El Niño, the thermocline is lifted up. This is due to the relaxation of the trade winds on the equator coupled with an Ekman divergence in the tropical zone induced by the presence of the intertropical convergence zone of the winds on the equator. High values of vertical velocities (more than 20 cm day^{-1}) are, however, confined to the 10°N to 10°S band.

INTRODUCTION

OF ALL the features related to El Niño phenomenon observed in the equatorial Pacific Ocean, the heat content change is one of the most obvious. Preceding El Niño, the heat content maximum is west of 180°; after El Niño, it lies mainly east of this longitude (HENIN and DONGUY, 1980). In the western Pacific, the wind field is different before and after El Niño; before El Niño, the intertropical convergence zone of the wind (ITCZ) moves seasonally from 10°N to 10°S and after El Niño, stays close to the equator (DONGUY and HENIN, 1981). Therefore, the relation between the change of heat content and the wind field needed investigation. KUTSUWADA (1981), with *Ryofu Maru* data gathered along 137°E, noted year-to-year variations of the thermal structures in the tropical north Pacific and concluded that they are related to changes of Ekman divergence. MEYERS (1975) related the annual variations of the geostrophic transports of the North Equatorial current to the divergence of Ekman transports in the eastern Pacific.

THERMAL STRUCTURE

In the tropical North Pacific, changes in the thermal structure have been described by MASUZAWA and NAGASAKA (1975), mainly in the years 1972 to 1973; at 137°E, anomalous cold water appeared in July 1972. According to WYRTKI (1979), the feature is due to a decrease of the mixed layer depth, which was estimated to be between 50 and 80 m in 1972 to

* Centre O.R.S.T.O.M. de Nouméa, B.P. A5 Nouméa, Nouvelle-Calédonie.

1973. HENIN and DONGUY (1980) have shown that this mechanism is responsible for the heat content changes in the equatorial Pacific.

Since 1969, the Centre O.R.S.T.O.M. de Nouméa has operated a surface monitoring program of the tropical Pacific using ships of opportunity, gathering surface temperature and salinity and wind speed and direction. In this study we have considered data collected between Noumea and Japan. Unfortunately, the data are poorly representative of the subsurface temperature. West of 180° the surface temperature is not a reliable indication of the subsurface thermal structure because of weak seasonal variations in temperature (28 to 30°C) from 10°S to 10°N (HENIN and DONGUY, 1979) and the poor accuracy (±0.5°C) of the measurements.

From 1965 to 1978, the hydrographic conditions were also monitored between 20°S and 5°N at approximately 170°E during cruises of the ORSTOM research vessel.

The results show year-to-year variations in the thermal structure of the upper layer. For example, from 5°N to 10°S there is a large difference between the mean thermal structure revealed by the BORA cruises in 1966 and that revealed by the CYCLONE cruises in 1967 (ROTSCHI, HISARD and JARRIGE, 1972). From the surface down to 200 m, the isotherms of the CYCLONE cruises are 50 m deeper than those of the BORA cruises (Fig. 1). To eliminate seasonal variations, BORA Cruise 2 in March 1966 and CYCLONE Cruise 2 in March 1967 can be compared with BORA Cruise 3 in July 1966 and CYCLONE Cruise 5 in July 1967 (Fig. 2). In both cases, the CYCLONE isotherms are deeper than those of BORA.

The hydroclimatic conditions differed between the two series of cruises. BORA cruises were just after the moderate 1965 El Niño and may be considered to show post-El Niño conditions: CYCLONE cruises were carried out before the weak 1969 El Niño and may be considered to show pre-El Niño conditions. During post-El Niño conditions, the isotherms are

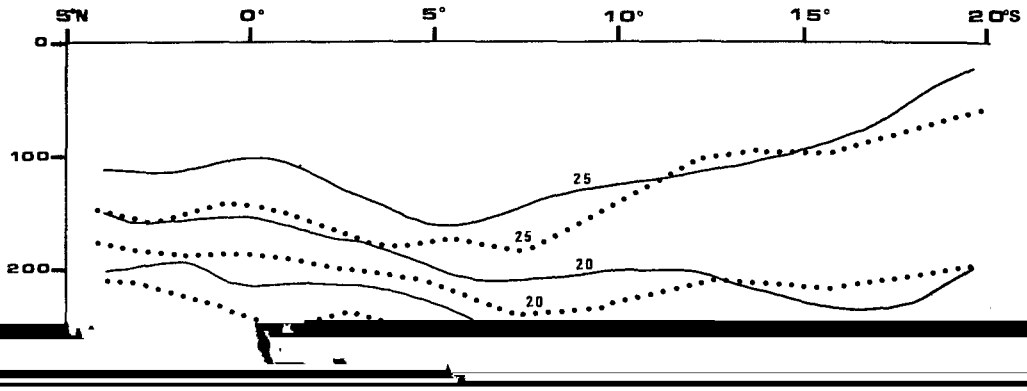

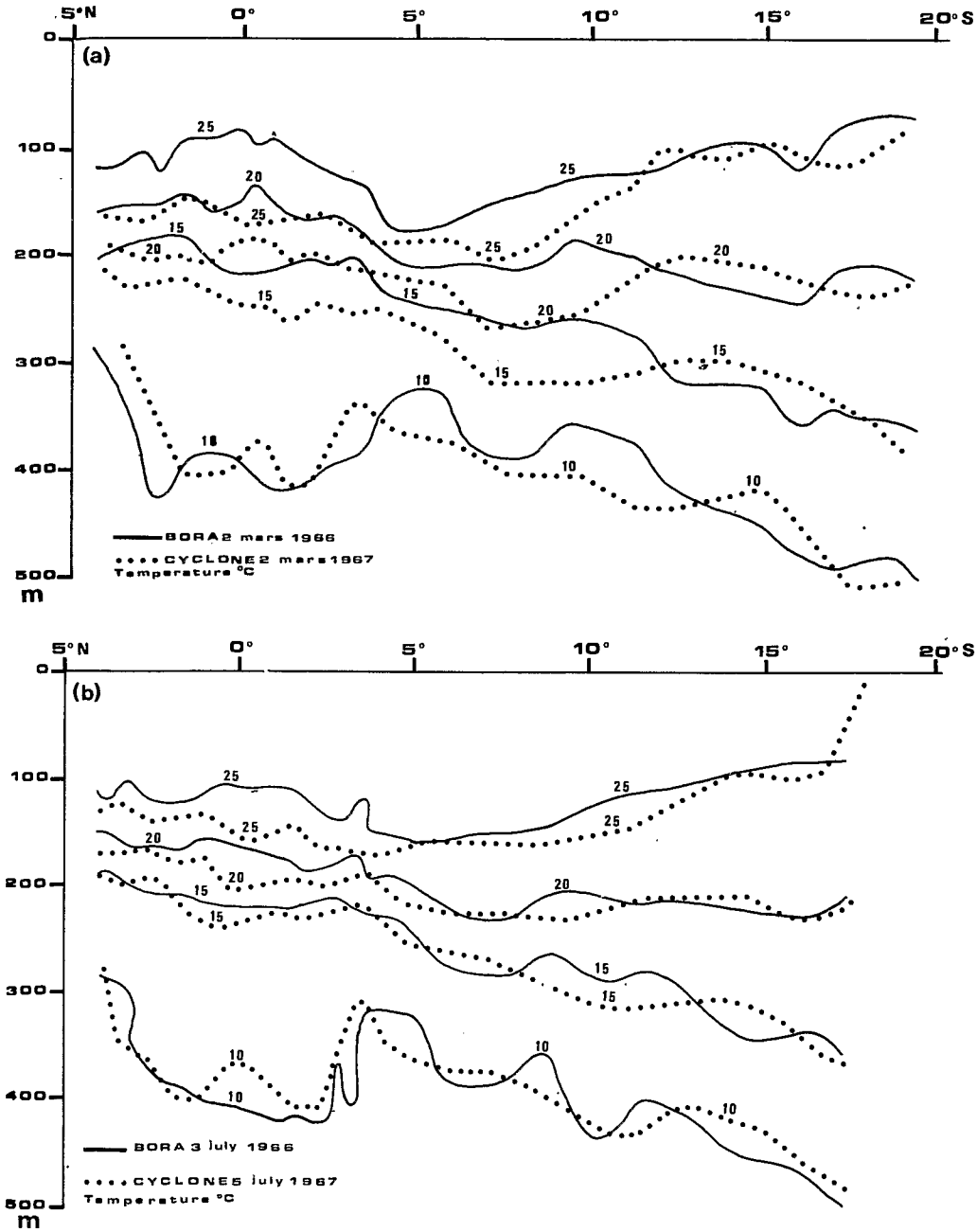

Fig. 2. Meridional distribution of temperature (°C) during the cruises BORA 2 (March 1966), CYCLONE 2 (March 1967), BORA 3 (July 1966), and CYCLONE 5 (July 1967).

shallower. This is also apparent on a time–space diagram (Fig. 3) showing the variations of the 25°C isotherm depth between 5°N and 20°S from 1965 to 1980. The 25°C isotherm represents almost the top of the thermocline. The following data available between 160°E and 180° have been used to draw the diagram: (a) hydrocasts from the Centre O.R.S.T.O.M. de Nouméa and from other laboratories (see Table 1) and (b) XBT data, mainly from the ORSTOM–CNEXO–Scripps monitoring program. The 25°C isotherm is deepest between 4 and 8°S. In this band, the thermocline depth was greater than 175 m during 1967 to 1968, 1971, and 1974 to 1975; from 5°N to 12°S, at the same times, the depth of the 25°C isotherm was more than 150 m. Conversely, during 1966, 1969 to 1970, 1973, and 1976 to 1980, the 25°C isotherm depth was usually between 150 and 175 m from 4 to 10°S and less than 150 m elsewhere. These periods followed the 1965, 1969, 1972, and 1976 El Niños. In post-El Niño hydroclimatic conditions, isotherms and thermocline are shallower and conse-

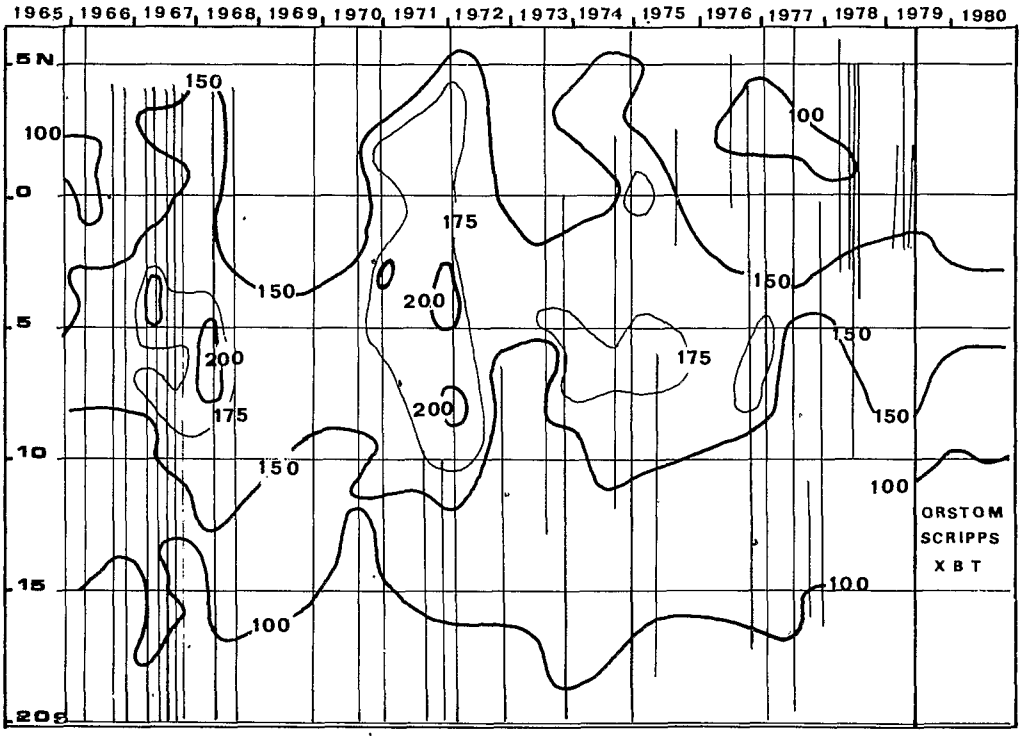

Fig. 3. Variations of the 25°C isotherm depth in meters, from data between 160°E and 180°. The cruises are marked by thin vertical lines.

WIND FIELD

Surface monitoring by ships of opportunity includes observations of the wind speed and direction. Since 1975, monthly charts drawn by the Centre O.R.S.T.O.M. de Nouméa show the wind field associated with surface conditions. After the 1976 El Niño, the ITCZ was close to the equator (Fig. 4). The changes in the wind field indicate that on both sides of the equator the divergence of Ekman transport can vary and consequently affect the depth of the surface layer. This effect may be defined as Ekman pumping.

The wind speed and direction have been observed along the Nouméa–Japan route. Between 1973 and 1978, four ships made such observations every 60 miles along routes passing through the Coral Sea and crossing the equator between 150 and 160°E. As a complete voyage lasts 40 days, the route has been run almost six times a month. After 1978, the route was run only twice a month.

The data were processed following the method of WYRTKI and MEYERS (1975) to compute the zonal and meridional components of the wind stress τx and τy, averaged by month and by degree of latitude. The drift current in the surface layer is considered and according to the Ekman theory the divergence of the horizontal mass transport is given by

$$\operatorname{div} M = \operatorname{curl} \frac{\tau}{f} = -\frac{\partial}{\partial x}\left(\frac{\tau y}{f}\right) - \frac{\partial}{\partial y}\left(\frac{\tau x}{f}\right), \quad \text{with } f = 2\,\omega \sin \phi. \tag{1}$$

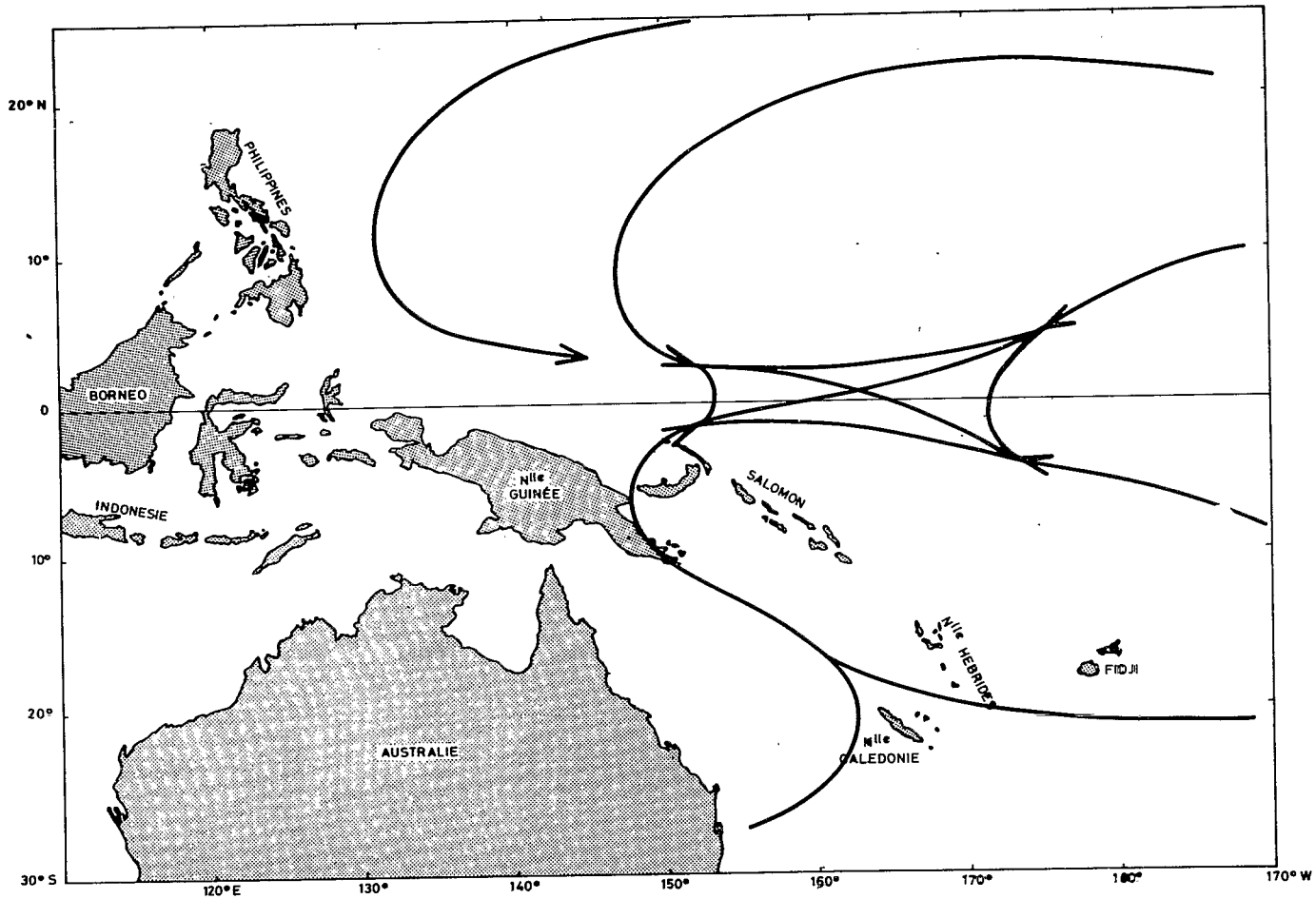

Fig. 4. Schematic wind field when the ITCZ is located on the equator during several months.

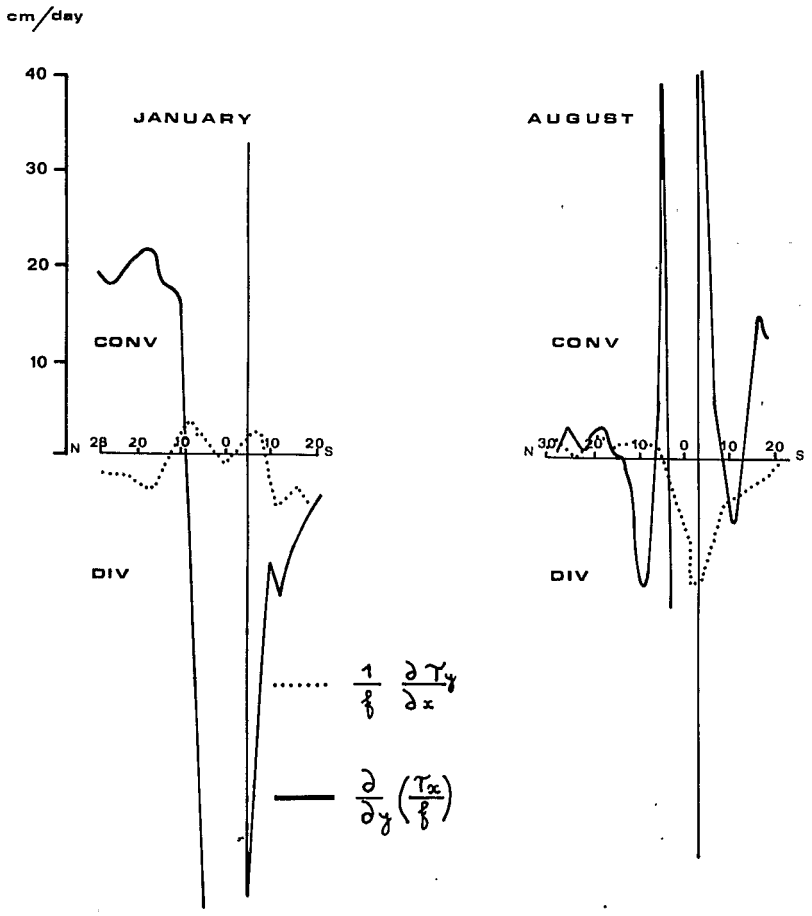

Fig. 5. Vertical velocity in centimeters per day of the two components of the Ekman pumping.

The effect of div M is called Ekman pumping, as div M can be expressed directly into upward or downward flow at the base of the Ekman layer according to the sign of the wind stress curl. Assuming that the zonal component of the Ekman transport is small in comparison with the meridional component, $\partial Mx/\partial x$ is neglected.

Equation 1 is then reduced to:

$$\operatorname{div} M = \frac{\partial My}{\partial y} = -\frac{\partial}{\partial y}\left(\frac{\tau x}{f}\right) = -\frac{1}{f}\frac{\partial \tau x}{\partial y} + \frac{\tau x}{fR \operatorname{tang} \phi}. \tag{2}$$

Using a finite difference method applied to a 1° latitude grid, equation 1 can be transformed to the following:

$$\frac{My_i - My_{i-1}}{l} = -\frac{1}{2\omega l}\left(\frac{\tau x_i}{\sin \phi_i} - \frac{\tau x_{i-1}}{\sin \phi_{i-1}}\right), \quad \text{with } l = 1°. \tag{3}$$

This takes into account both the wind stress curl effect and the planetary curl effect, which are of great importance close to the equator.

Due to insufficient sampling, high short-scale variability remained in the data and a strong low-pass filtering appeared necessary. A time–space three-point running mean of triangular shape was used. In addition, the data of each month-degree square were weighted by the number of observations included, and a test suppressed the spike influences (see Appendix). This processing was applied twice before the curl calculation and had to be repeated three times more after the calculation until coherent patterns appeared.

The zonal derivative of the meridional wind stress has been neglected in the calculation of div *M*. Although this assumption was often made in the central Pacific, it is more questionable in the western equatorial Pacific, where under the consecutive influence of the west winds during the West Monsoon period (January to March), strong zonal gradients of wind stress may occur mainly south of the equator. With data from WYRTKI and MEYERS (1975), the

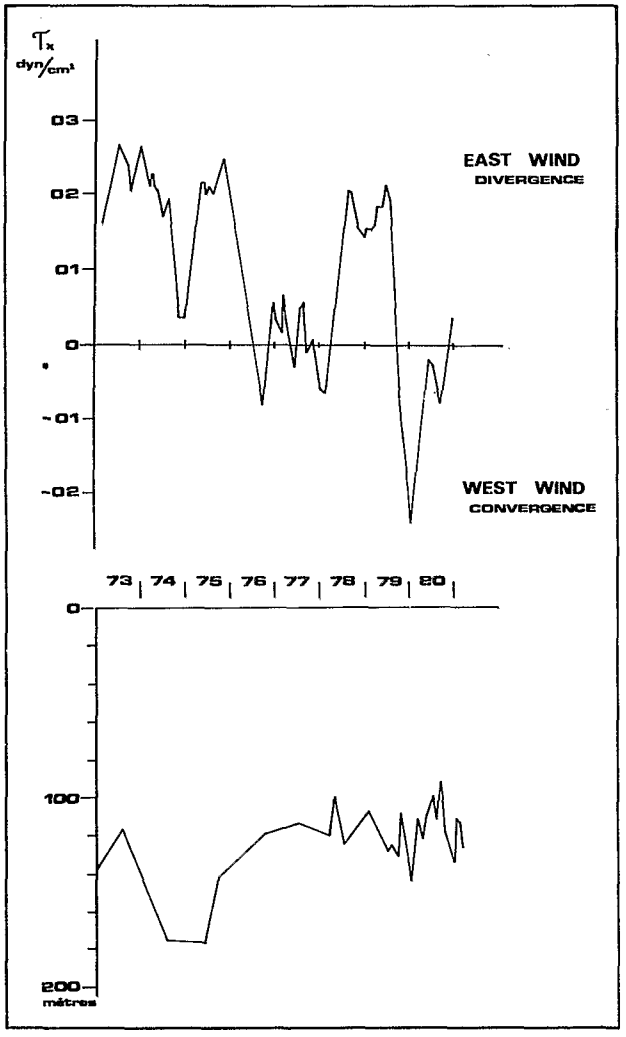

Fig. 6. Zonal wind stress (dyn cm^{-2}) at the equator and the depth of the 25°C isotherm (m).

extreme situations of January and August have been examined. In Fig. 5, the result of the computation of the two components of the Ekman pumping in the 140 to 160°E band with a 3°N to 3°S interruption is expressed in meters per day. Usually, vertical motion due to the zonal gradient of Ekman transport is weak in comparison with that due to the meridional gradient of Ekman transport induced by the north to south variations of the zonal wind stress and of the Coriolis parameter, except during August. During August, north of 15°N latitude, the two components have the same order of magnitude but they are very weak. In one part of the southern hemisphere, the two components act in opposite directions. However, the data are long-term means and for individual years greater differences may occur.

In the present study, to eliminate the equatorial effect, the curl computation was not undertaken between 1° 30′N and 1° 30′S. However, MEYERS (1978) showed that Ekman pumping is not valid between 4°N and 4°S; the large values of velocity calculated close to the equator are probably not realistic but are induced mainly by small values of the Coriolis parameter. But MEYERS (1978), using a model including friction (GILL, 1975) provided also for the annual variations and large vertical velocities (35 m per month), which are not consistent with the observed isotherm displacement. Consequently, to present a qualitative index of the strength of the divergences or convergences found strictly at the equator, the zonal wind stress has been averaged into the 1°S to 1°N band (Fig. 6).

RELATIONS BETWEEN WIND AND THERMAL STRUCTURE

At the equator, the Ekman transport divergence is roughly proportional to the local zonal wind stress (GILL, 1975). In the present case (Fig. 6) the zonal wind stress seems really associated with the vertical movement of the 25°C isotherm. From 1973 to 1976, east wind prevailed and induced equatorial divergence associated with a deepening of the 25°C isotherm. Conversely, from 1976 to 1980, the wind was mostly westerly except during part of 1978 and 1979 and induced equatorial convergence associated with a shoaling of the 25°C isotherm. These paradoxical features are in accordance with WYRTKI's (1979) statements: in a pre-El Niño period, strong easterly winds blowing along the entire equatorial Pacific induce a piling up of the water in the western Pacific and high sea level. Due to the baroclinic balance, isotherms deepen. Conversely, weak easterly or westerly winds induce low sea level and, by baroclinic balance, a lifting up of the isotherms in the western Pacific. This is characteristic of a post-El Niño period. However, as this baroclinic motion is due to the equatorial wind field across all the Pacific, it may not be related to the local wind, if this wind is not correlated by itself with that of the central Pacific. This occurred in 1978 to 1979, when east winds prevailed at 160°E, but they were poorly correlated with the wind observed near 160°W, using data obtained by ships of opportunity and from SADLER and KILONSKY (1981).

Figure 7 is a space–time diagram showing the 1973 to 1980 pattern of divergence (positive values) or convergence (negative values) due to the Ekman pumping as previously computed. There are several permanent features. From 15 to 25°N there is usually a convergence coinciding with the boundary between the North Equatorial Current and the North Tropical Countercurrent. Between 5 and 10°N a divergence appears at the limit of the North Equatorial Current and the North Equatorial Countercurrent. At 5°N, a convergence is at the boundary between the North Equatorial Countercurrent and the Equatorial Current. South of the equator, similar permanent features appear at 5°S, convergence between the Equatorial Current and South Equatorial Countercurrent, and at 10°S, a divergence (sometimes called the Divergence of the Solomons) between the South Equatorial

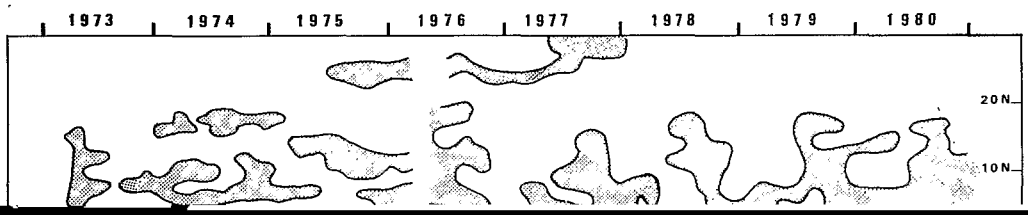
1973
1974
1975
1976
1977
1978
1979
1980
20N
10N

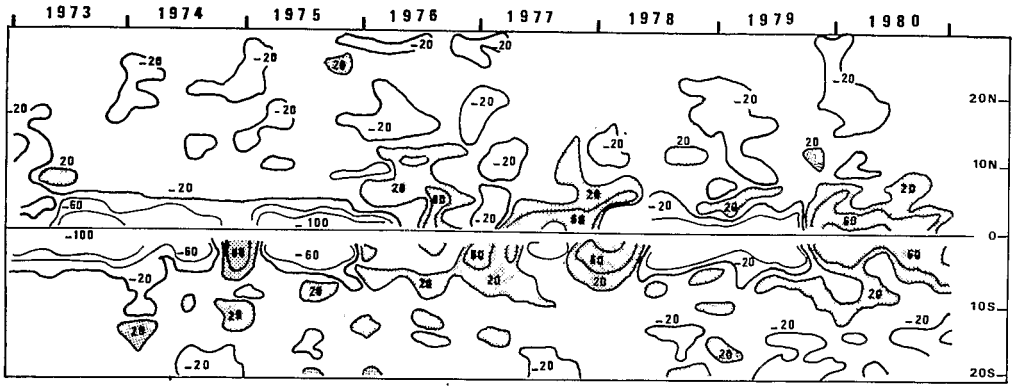

Fig. 8. Vertical velocity in centimeters per day. Only velocities of more than 20 cm per day are indicated.

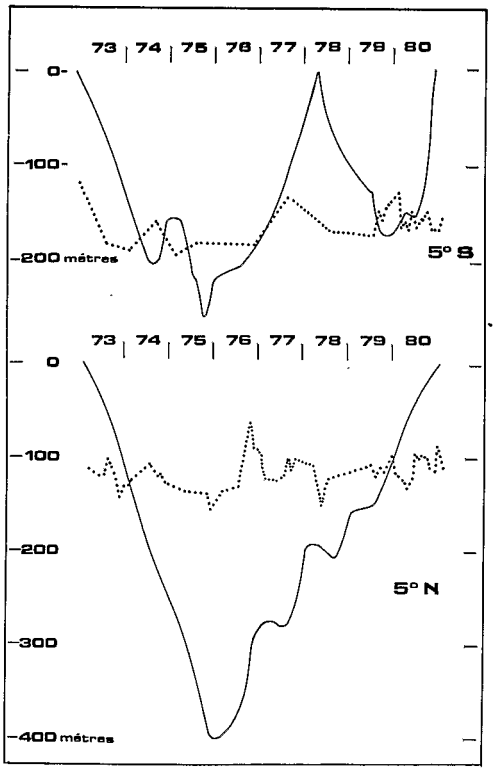

Fig. 9. Vertical displacement due to Ekman pumping (full line) and depth of the 25 °C isotherm (dotted line) at 5°S and 5°N.

large velocity and great displacement* in the Ekman pumping. The Ekman pumping also differed at 5°S and at 5°N. At 5°N, there was one oscillation between 1973 and 1980, whereas at 5°S two are evident, one from 1973 to 1978, the other from 1978 to 1980. One

* It is obvious that for long-term fluctuations in the case of quasi-permanent downward velocities; the isotherms cannot deepen indefinitely and that, after a few months, a new equilibrium state must be reached between Ekman pumping and geostrophic divergence.

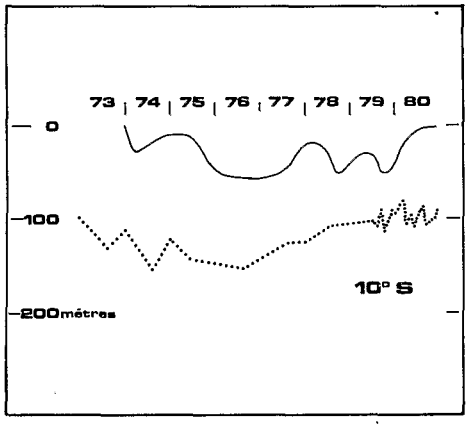

Fig. 10. Vertical displacement due to Ekman pumping (full line) and depth of the 25°C isotherm (dotted line) at 10°S.

can infer that, as already noted for the central Pacific (SADLER and KILONSKY, 1981) significant differences must occur between the trade wind field anomalies in both hemispheres.

At 10°S (Fig. 10), vertical displacement computed from Ekman pumping is consistent with the observed depth change of the 25°C isotherm. Negative displacement and 25°C isotherm deepening of the same magnitude are observed before 1976. After this date, the displacement due to Ekman pumping is positive and the 25°C isotherm is lifted up.

The vertical displacement of the 25°C isotherm induced by Ekman pumping on each side of the equator (Figs 9, 10) and the vertical displacement of the 25°C isotherm due to baroclinic balance on the equator (Fig. 6) are approximately in phase: before El Niño, isotherms deepen, whereas after El Niño, they shoal.

DISCUSSION

The role of Ekman pumping in the variations of the tropical current system has been emphasized by several authors. However, the studies mainly deal with seasonal cycles. In the eastern Pacific, MEYERS (1975) showed that the local wind stress curl could explain the seasonal variation of the North Equatorial Current. In the central and western Pacific, WHITE (1977) demonstrated that the combination of the Rossby waves generated at the eastern boundary with the local atmosphere forcing induces baroclinic long waves propagating westward. Consequently, the baroclinic structure does not fluctuate in phase with the local annual wind forcing. Furthermore, the amplitude of these waves increases toward the equator. On the other hand, SCHOPF (1980) pointed out the dominant role of Ekman transport in the process of heat storage between the equator and 10° latitude.

In the case of the western Pacific, the seasonal variation of the thermal structure is very weak. MEYERS (1979) found an amplitude of less than 6 m for the annual depth variation of the 14°C isotherm on the equator at 160°E. Near 150°E, according to MEYERS, WHITE and HASUNUMA (1981), the annual temperature variation has a maximum amplitude of about 1.5°C at the equator and at 150-m depth, that would yield an annual isotherm displacement of about 10 m within the depth range of the main thermocline. By comparison with results

from WHITE and HASUNUMA (1980), this effect has roughly the same magnitude as the interannual standard deviation. However, in the present study, it appears that both equatorial isotherm displacement (Fig. 6) and Ekman pumping effects (Figs 9 and 10) are dominated by long-term fluctuations and that the annual variation can be neglected as a first approximation.

CONCLUSION

In the western Pacific, before El Niño, the deepening of the thermocline observed at the equator is considered to be the baroclinic response to an elevation of sea level induced by the strengthening of the trade winds. The feature can extend on each side of the equator as far as 10° latitude by Ekman convergence induced by wind forcing. After El Niño, the intertropical convergence zone of the wind changes from its usual location at 15°S in the southern summer and at 15°N in the northern summer to a location over the equator, west of 180°. The relaxation of the trade wind results in a lifting up of the equatorial isotherms. The new wind field induces an Ekman divergence in the tropical area and consequently a lifting up of thermocline and isotherms. This occurred in the case of the 1976 El Niño.

As a first approximation the strength and duration of the Ekman pumping does not seem to be related to the intensity of the previous El Niño. Thus in 1973, after the strong 1972 El Niño, no Ekman pumping was detected. This accords with the quick dissipation in spring 1973 of the large-scale negative anomaly of temperature in the subsurface (WHITE and WYLIE, 1977). Conversely, the moderate 1976 El Niño was followed by a long period of Ekman pumping between 10°N and 10°S from 1976 to 1981, inducing a lifting up of the isotherms from their mean positions.

On the other hand, in the western equatorial Pacific the upwelling effect due to the local wind and the baroclinic effect act in opposite directions on the thermocline and isotherm depths. For the long-term variations, the baroclinic effects prevail and induce isotherm deepening with trade wind forcing. For the short-term fluctuations, it is likely that the local divergence effect predominates and induces an inverse situation, as suggested by anomalies observed in the relation between wind stress at the equator and isotherm depth. In any case, phase differences must be observed between the two phenomena, the upwelling response being faster than the baroclinic one. However, the wind data used in this study are too sparse to solve this problem. It would be desirable that in addition to the thermal observations, there were special studies of surface winds in the western Pacific.

APPENDIX

Data filtering

The filter used is a classical "hanning" on three points $(\frac{1}{4}, \frac{1}{2}, \frac{1}{4})$. The data are equally weighted on the space and time axes, i.e., each datum is replaced by a weighted average using the four closest points on the time and latitude axes. Furthermore, the data are weighted by the number of observations collected in each grid mesh and a test is applied to avoid the leakage of spikes and erroneous values. The complete formula is:

$$T_{ij} = \frac{\sum_{h,k=-1}^{h,k=+1} \alpha_{(i+h)(j+k)} n_{(i+h)(j+k)} \tau_{(i+h)(j+k)} \partial_{(ijhk)}}{\Sigma n_{(i+h)(j+k)} \alpha_{(i+h)(j+k)}}$$

with T_{ij} the filtered monthly wind stress value for latitude i and month j, τ_{ij} the original monthly zonal wind stress, n_{ij} the number of observations in the month-degree square, and $\alpha_{(i+h)}(j+k)$ weights with $\alpha_{ij} = 1$ for $h = k = 0$, $\alpha = \frac{1}{4}$ for $h = k = +1$, ∂_{ij} test based on the gradient of wind stress between the central and neighbouring points with

$$\partial_{ij} = 0 \text{ for } |\tau_{ij} - \tau_{(i+h)(j+k)}| > E \frac{n_{ij}}{n_{(i+h)(j+k)}}$$

$$\partial_{ij} = 1 \text{ for } |\tau_{ij} - \tau_{(i+h)(j+k)}| < E \frac{n_{ij}}{n_{(i+h)(j+k)}} .$$

The value of E was arbitrarily fixed at $20\,m^2\,s^{-2}$.

The same filter was applied to the computed curl with the following modifications: the number of observations is no longer taken into account and the value used for the gradient test is fixed at $E = \Delta\nu = 5$ m day^{-1}.

REFERENCES

DONGUY J. R. and C. HENIN (1981) Two types of hydroclimatic conditions in the south western Pacific. *Oceanologica Acta*, **4**, 57–62.

GILL A. E. (1975) Models of equatorial currents. Proceedings of the Symposium on Numerical Models of Ocean Circulation, Durham N. H. 1972, U.S. National Academy of Science, pp. 181–203.

HENIN C. and J. R. DONGUY (1979) Sea surface salinity and temperature anomalies between Japan and New Caledonia (1969–1978). Proceedings of the 4th C.S.K. Symposium, Tokyo 1979, pp. 321–331.

HENIN C. and J. R. DONGUY (1980) Heat content changes within the mixed layer of the equatorial Pacific Ocean. *Journal of Marine Research*, **38**, 767–780.

KUTSUWADA K. (1981) Temperature variations in the N.W. Pacific–Tropical Ocean. Atmosphere Newsletter, 6. (Unpublished Manuscript.)

MASUZAWA J. and K. NAGASAKA (1975) The 137°E oceanographic section. *Journal of Marine Research*, Supplement 33, pp. 109–116.

MEYERS G. (1975) Seasonal variation in transport of the Pacific North Equatorial Current relative to the wind field. *Journal of Physical Oceanography*, **5**, 442–449.

MEYERS G. (1978) Annual variation in the depth of 14°C in the Tropical Pacific Ocean. Ph.D. Dissertation, University of Hawaii, 79 pp.

MEYERS G. (1979) Annual variation in the slope of the 14°C isotherm along the equator in the Pacific Ocean. *Journal of Physical Oceanography*, **9**, 885–891.

MEYERS G., W. WHITE and K. HASUNUMA (1981) Annual variation in baroclinic structure of the northwestern Tropical Pacific. *Oceanographie Tropicale*, **1**, No. 1.

ROTSCHI H., P. HISARD and F. JARRIGE (1972) Les eaux du Pacifique occidental à 170°E entre 20°S et 4°N. Travaux et Documents de l'ORSTOM, **19**, 113 pp.

SADLER J. C. and B. J. KILONSKY (1981) Trade wind monitoring using satellite observations. Pub. U.H. MET 81-